Eurasian J. Sci. Eng., 20xx, 11(3), 49-65
https://doi.org/10.23918/eajse.v11i3p4

Published by Tishk International University
Available at: https://eajse.tiu.edu.iq/

RESEARCH ARTICLE Open Access

A Multifaceted Study of COVID-19: Stability Analysis, Numerical Solution, and Sensitivity Analysis

Hemn Mohammed Rasool [1]*, Berivan Faris Azeez [1], and Mardan Ameen Pirdawood [1]

[1] Department of Mathematics, Faculty of Science and Health, Koya University, Koya 44023, Kurdistan Region - F.R. Iraq.

Article History
Received: 29.12.2024
Revised: 16.09.2025
Accepted: 23.11.2025
Published: 27.11.2025
Communicated by: Asst. Prof. Dr. Salisu Ibrahim
Email address:
hemn.mohammed@koyauniversity.org
Corresponding Author

Abstract: The COVID-19 epidemic has emerged as a significant worldwide health concern, necessitating a thorough analysis of medical data pertaining to the virus. This research highlights the need to use mathematical modeling and computer simulations to comprehend fundamental transmission properties on a nationwide level. To efficiently control illnesses, it is essential to include computational methodologies and behavioral evaluations into the mathematical equations of the model. This article analyzes the model of the coronavirus, beginning with significant global healthcare challenges and offering essential guidance. The objective of the research is to investigate the COVID-19 case model in Nigeria for the year 2020, using approaches to ascertain the existence and uniqueness of the system's solution. The Implicit-Explicit Runge-Kutta (4,5,5) method was used for numerical computations, stability assessment, and sensitivity analysis. The Implicit-Explicit Runge-Kutta methods are often used as computing techniques for solving differential equations. Furthermore, the classical Runge-Kutta techniques are also used to solve intricate differential equations to see the efficiency of our technique. The data acquired via these procedures provide vital insights into the worldwide epidemic. These models have the capacity to forecast forthcoming data pertaining to persons who are ill, susceptible, socially isolated, and have recovered. This adds to worldwide endeavors in enhancing preventative measures and intervention initiatives. Stability analysis is used to identify crucial locations where disease transmission may be halted, while sensitivity analysis assesses the unique sensitivities of each component of the model to factors such as full, half, and non-normalizations. The results indicate that nearly every parameter in the model affects the spread of the virus among susceptible, exposed, and separated people.

Keywords: *Mathematical Modeling; COVID-19 Disease; Stability Analysis; Implicit-Explicit Runge-Kutta Method; Sensitivity Analysis.*

1. Introduction

A mathematical model serves as a precise mathematical depiction of real-world phenomena, employing symbols, equations, and formulae to encapsulate intricate processes. Given the substantial global health impact, it is imperative to gain a comprehensive understanding of and the ability to predict the behavior of emerging coronaviruses, such as COVID-19. Many researchers in the mathematical, computational, clinical, and investigative fields have worked to model, predict, treat, and mitigate the effects of this disease. The scientific community can, however, always do better. The relevance of mathematical and computational models for predicting the dynamics of new coronavirus diseases has increased in recent years, prompting a plethora of publications in this area. World health officials were alarmed when the COVID-19 epidemic broke out in the Chinese city of Wuhan in the province of Hubei in the latter half of 2019. In the year that followed, the epidemic had reached nearly every corner of the world [1].

In Wuhan, China, there was a brief period characterized by a succession of perplexing health problems, including unexplained instances of coughing, pneumonia, difficulty breathing, exhaustion, and high

body temperature. The occurrence of these mysterious diseases led to a sequence of activities, such as the shutdown of establishments, educational institutions, and markets, as well as the imposition of regulations on social engagements, curfews, lockdowns, and constraints on gatherings, among other interventions [2]. Nigeria has been affected by the repercussions of the COVID-19 pandemic. The first instance of COVID-19 was officially verified in Lagos State, situated in the southern region of Nigeria, on February 27, 2020. The outbreak in the country started when an Italian individual landed in Nigeria on February 24, 2020. This person sought medical assistance on February 26, 2020, marking the first known case in Nigeria (refer to Fig. 1) [3].

According to the arrival of the COVID-19 pandemic in Nigeria, the national government, as well as several state authorities, established distinct medical organizations and isolation centers as proactive measures to combat and manage the transmission of the virus. The Nigerian Center for Disease Control (NCDC), a governmental entity, disseminated essential public health information to the Nigerian people. This guide included details on symptom recognition, the distribution of vital information, and methods for preventing the disease. The NCDC created extensive national and sub-national organizations of health service professionals, enhancing the country's ability to effectively conduct contact surveillance and handle cases. Also, the NCDC did a lot of work to make sure that research labs could handle more work so that they could step up their pandemic diagnostic game. The goal of these concerted actions was to make Nigeria more resilient in the face of the unprecedented health calamity that COVID-19 posed. Since the COVID-19 outbreak started, mathematicians have been increasingly used by researchers to help better grasp it. Using such models, one may investigate the dynamics of the epidemic's progress, the virus's spread, its impacts on individuals, control and preventive strategies, and the effectiveness of these actions. New investigations in this area, as shown in the references [4], have significantly increased our understanding of the subject. The features and distribution of COVID-19 throughout Lagos, Nigeria, were examined in a research by Okuonghae and Omame [5]. At the same time, Roseline and colleagues [6] estimated the pandemic-related death toll in Nigeria using linear regression, a statistical approach. Adegboye and colleagues [7] also looked at how COVID-19 spread from its initial transmission to Nigeria. Ajisegiri et al. [8] conducted a comprehensive investigation on the COVID-19 epidemic in Nigeria. Researchers from several disciplines have conducted crucial research into prospective therapies and preventive measures to alleviate the impact of the epidemic, and the results have shown promise. However, it is crucial to conduct a thorough study of the most recent models and deliver a reasonable and complete appraisal of the present circumstances.

Despite the numerous modeling approaches suggested for predicting the progression of new coronavirus infections, it is evident that this area needs development. The findings are anticipated to be of superior quality if the models are formulated based on mass action laws, consist of reaction rate constants, and evaluate the sensitivity of every state to the model parameters [9]. The complexity involved in solving systems of ordinary differential equations often results in a lack of exact analytical solutions for most of these issues. Moreover, these obstacles are exacerbated by the coexistence of several temporal scales that develop concurrently inside these issues, despite the numerous documented methodologies for reducing models aimed at minimizing complexity and deriving analytical solutions [10, 11], but numerical techniques are required for solving such problems. Consequently, several scholars have shown a strong interest in investigating these complexities. As a result, a wide range of numerical approaches have developed throughout time. The techniques used in this context include the techniques Euler method, the Runge-Kutta scheme, the Implicit-Explicit (IMEX) Runge-Kutta scheme, the Singly Diagonally Implicit Runge-Kutta (SDIRK) approaches, and the Semi-Implicit and Explicit Runge-Kutta approaches. The Implicit-Explicit Runge-Kutta scheme (IMEX-RK (4,5,5)) is a popular method for solving differential equation systems (1). This method is

significant because practical data shows it solves difficult problems. References [12, 13] provide further information on these approaches and their practical applications.

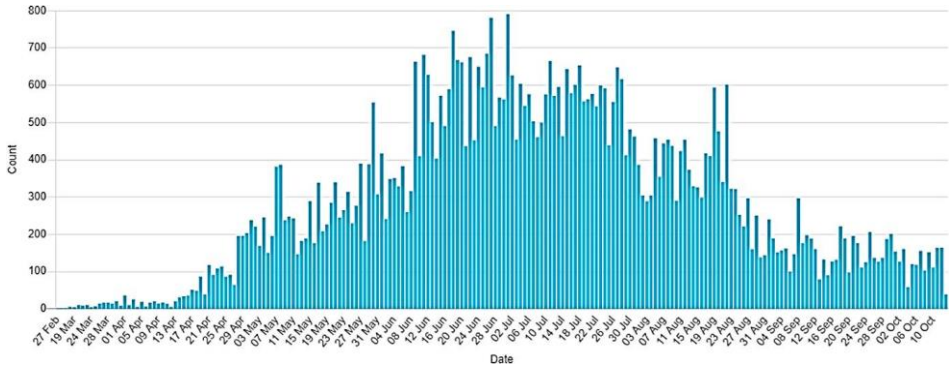

Figure 1: Confirmed COVID-19 Cases-Nigeria 2020 (3).

2. Mathematical Modeling for the COVID-19 Disease

This study examines a theoretical framework for comprehending the transmission rates of the coronavirus (COVID-19) illness, grounded in basic principles. Propose a dynamic model to depict the progression of the human population in relation to the COVID-19 pandemic. Define $N(t)$ as the cumulative human population at a given time t. Individuals can be classified into six distinct groups: susceptible individuals $(S(t))$, exposed individuals $(E(t))$, asymptotically infected individuals $(I_A(t))$, symptomatic infected individuals $(I_S(t))$, individuals in quarantine $(Q(t))$, and individuals who have recovered or been removed from COVID-19 $(R(t))$. By using this classification, we can represent the overall population at a certain moment as the cumulative sum of these six classifications: $N(t) = S(t) + E(t) + Q(t) + I_A(t) + I_S(t) + R(t)$. This formulation enables us to monitor and study the population's dynamics within the framework of the COVID-19 pandemic, including the different phases of infection and recovery. The natural birth rate and mortality rate for humans are represented by r_1 and r_2, respectively. Individuals who are susceptible (S) may transition to the infected condition (E) after being adequately exposed at a rate of r_3. Alternatively, they may transfer to the quarantined class at a rate of r_4. There are three potential outcomes for exposed people (E): they may change to the quarantined class (Q) at a rate of r_5, become infected asymptomatically (I_A) at a rate of r_7, or get infected symptomatically (I_S) at a rate of r_6. Individuals in the quarantined state (Q) may also be verified as infectious, either with symptoms (I_S) or without symptoms (I_A), at rates of r_8 and r_9, respectively. The recovery rate for persons who are infected but show no symptoms (I_A) is denoted as r_{12}, whereas the recovery rate for those who are infected and show symptoms (I_S) is denoted as r_{11}. Natural mortality, represented by the parameter r_2, may cause a decline in the population of each of these groups. Additionally, the population of persons infected with symptoms (I_S) can be reduced by death caused by the sickness at a specified rate. The infected class of people without symptoms (I_A) does not include mortality because of the illness. This model fails to include the possibility of reinfection after the process of healing. Figure 2 displays the schematic design depicting the transmission of COVID-19. Table 1 contains an extensive compilation of biologically significant parameters and their respective values. The model's system of differential equations is expressed in system (1).

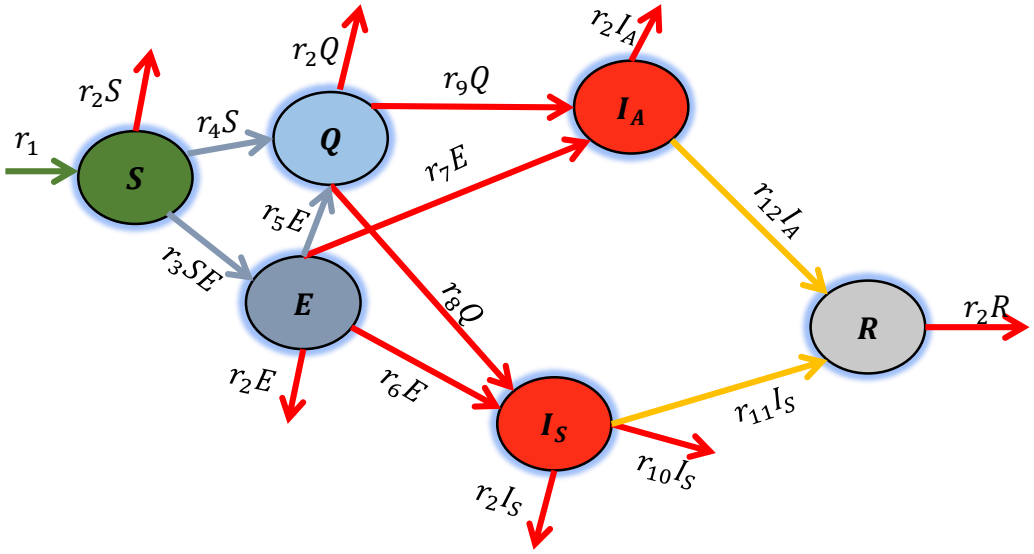

Figure 2: The model examines the interactions between individuals and the transmission rates of the coronavirus disease (COVID-19) [3].

$$
\begin{aligned}
\frac{dS(t)}{dt} &= r_1 - (r_4 + r_2)S(t) - r_3S(t)E(t),\\
\frac{dE(t)}{dt} &= r_3S(t)E(t) - (r_5 + r_2 + r_6 + r_7)E(t),\\
\frac{dQ(t)}{dt} &= r_4S(t) + r_5E(t) - (r_2 + r_8 + r_9)Q(t),\\
\frac{dI_A(t)}{dt} &= r_7E(t) + r_9Q(t) - (r_2 + r_{12})I_A(t),\\
\frac{dI_S(t)}{dt} &= r_6E(t) + r_8Q(t\,) - (r_{10} + r_2 + r_{11})I_S(t),\\
\frac{dR(t)}{dt} &= r_{12}I_A(t) + r_{11}I_S(t) - r_2R(t).
\end{aligned} \tag{1}
$$

With initial conditions:

$$\big(S(0), E(0), Q(0), I_A(0), I_S(0), R(0)\big) = (0.5, 0.2, 0.1, 0.2, 0.1, 0). \tag{2}$$

Table 1: Set of parameters with their biological meanings [3].

Parameter	Description	Values
r_1	Recruitment (natality) rate	0.02537
r_2	Natural mortality rate	0.0106
r_3	The contact rate between individuals who are susceptible to a particular infection and those who have been exposed to it plays a crucial role in the transmission dynamics of the disease.	0.0805
r_4	Transfer rate from susceptible individuals to quarantine	0.0002
r_5	The rate of exposed people being transferred to quarantine	$2.0138e-4$
r_6	Rate of transition from the exposed population to the symptomatic infected population.	0.4478
r_7	The transition rate from the group of individuals who have been exposed to the class of asymptomatic individuals.	0.0668

r_8	The transition rate from the quarantined population to the symptomatic infected category.	$3.2084e-4$
r_9	The ratio of individuals placed in quarantine to those who are asymptomatic and infected is a crucial metric in assessing the effectiveness of public health measures.	0.0101
r_{10}	Coronavirus-related mortality rate in the class of those who are symptomatic and infected.	$1.6728e-5$
r_{11}	Recovery rate of those with symptoms of infection.	$1.6728e-5$
r_{12}	Recovery rate of asymptomatic infected individuals	$5.7341e-5$

3. Existing and Uniqueness Solution for the System

To apply the numerical methods to any system of differential equations, first, we have to show that this system has a unique solution. Here we prove that the solution of system (1) exists and is also unique based on the Picard-Lindelöf theorem [14], The Picard-LindelöThe theorem states that if the right-hand side of an ODE system is Lipschitz continuous and continuous with respect to the dependent variables, then there exists a unique solution to the initial value problem. Consider the system of DEQ (1) with initial conditions given in (2). Let us define the vector of components and the vector field $F(C)$ represents the system (1):

$$C(t)=\begin{pmatrix}S(t)\\E(t)\\Q(t)\\I_A(t)\\I_S(t)\\R(t)\end{pmatrix},\quad F(C)=\begin{pmatrix}r_1-(r_4+r_2)S-r_3SE\\r_3SE-(r_5+r_2+r_6+r_7)E\\r_4S+r_5E-(r_2+r_8+r_9)Q\\r_7E+r_9Q-(r_2+r_{12})I_A\\r_6E+r_8Q-(r_{10}+r_2+r_{11})I_S\\r_{12}I_A+r_{11}I_S-r_2R\end{pmatrix}.$$

Based on the definition of a polynomial function, each component of $F(C)$ is a polynomial in S,E,Q,I_A,I_S, and R. And polynomials are continuous functions. Therefore, $F(C)$ is continuous. In order to verify Lipschitz continuity, it is necessary to demonstrate the existence of a constant L that is sufficient for every pair of vectors C_1 and C_2,

$$\|F(C_1)-F(C_2)\|\le L\|C_1-C_2\|.$$

Let us define the Jacobian matrix for $F(C)$ as follows:

$$\text{Jacobian}(F)=\begin{bmatrix}\frac{\partial f_1}{\partial S}&\frac{\partial f_1}{\partial E}&\frac{\partial f_1}{\partial Q}&\frac{\partial f_1}{\partial I_A}&\frac{\partial f_1}{\partial I_S}&\frac{\partial f_1}{\partial R}\\\frac{\partial f_2}{\partial S}&\frac{\partial f_2}{\partial E}&\frac{\partial f_2}{\partial Q}&\frac{\partial f_2}{\partial I_A}&\frac{\partial f_2}{\partial I_S}&\frac{\partial f_2}{\partial R}\\\frac{\partial f_3}{\partial S}&\frac{\partial f_3}{\partial E}&\frac{\partial f_3}{\partial Q}&\frac{\partial f_3}{\partial I_A}&\frac{\partial f_3}{\partial I_S}&\frac{\partial f_3}{\partial R}\\\frac{\partial f_4}{\partial S}&\frac{\partial f_4}{\partial E}&\frac{\partial f_4}{\partial Q}&\frac{\partial f_4}{\partial I_A}&\frac{\partial f_4}{\partial I_S}&\frac{\partial f_4}{\partial R}\\\frac{\partial f_5}{\partial S}&\frac{\partial f_5}{\partial E}&\frac{\partial f_5}{\partial Q}&\frac{\partial f_5}{\partial I_A}&\frac{\partial f_5}{\partial I_S}&\frac{\partial f_5}{\partial R}\\\frac{\partial f_6}{\partial S}&\frac{\partial f_6}{\partial E}&\frac{\partial f_6}{\partial Q}&\frac{\partial f_6}{\partial I_A}&\frac{\partial f_6}{\partial I_S}&\frac{\partial f_6}{\partial R}\end{bmatrix}. \tag{3}$$

$$(4) \quad \text{Jacobian}\,(F) = \begin{bmatrix} -r_4 - r_2 - r_3E & -r_3S & 0 & 0 & 0 & 0 \\ r_3E & r_3S - r_5 - r_2 - r_6 - r_7 & 0 & 0 & 0 & 0 \\ r_4 & r_5 & -r_2 - r_8 - r_9 & 0 & 0 & 0 \\ 0 & r_7 & r_9 & -r_2 - r_{12} & 0 & 0 \\ 0 & r_6 & r_8 & 0 & -r_{10} - r_2 - r_{11} & 0 \\ 0 & 0 & 0 & r_{12} & r_{11} & -r_2 \end{bmatrix}$$

Next, we find the Lipschitz constant L by applying the following formula:

$$L = \max\left(\sum_{j=1}^{6} \left|\frac{\partial f_i}{\partial c_j}\right|\right) \text{ for } i = 1,2,\dots,6.$$

By definition, we have $S, E \geq 0$, then for $i = 1$, the part of f_1 is $|-(r_4 + r_2) - r_3E\ | + |-r_3S| + 0 + 0 + 0 + 0 = r_4 + r_2 + r_3E + r_3S$, then $f_1 = r_4 + r_2 + r_3(E + S)$, in the same way for $i = 2,3,4,5$ we conclude that $(f_2, f_3, f_4, f_5, f_6) = (r_3E + r_3S + (r_5 + r_2 + r_6 + r_7), r_4 + r_5 + r_2 + r_8 + r_9, r_7 + r_9 + r_2 + r_{12}, r_6 + r_8 + r_{10} + r_2 + r_{11}, r_{12} + r_{11} + r_2)$, then, the Lipschitz constant is $L = \max(f_1, f_2, f_3, f_4, f_5, f_6)$. And by substituting the values of S and E , from equation (2), L becomes

$$L = \max(r_2 + (0.7)r_3 + r_4, r_2 + (0.7)r_3 + r_5 + r_6 + r_7, r_2 + r_4 + r_5 + r_8 + r_9, r_2 + r_7 + r_9 + r_{12}, r_2 + r_6 + r_8 + r_{10} + r_{11}, r_2 + r_{11} + r_{12}).$$

The partial derivatives are bounded because all the r_i values are constant, as seen in Table 1. Thus, the existence of this constant L guarantees that the Lipschitz condition is met. We proved that $F(C)$ is continuous and satisfies the Lipschitz condition, then by Picard-Lindelöf theorem, the solution of the system (1) exists, and it is unique $t = 0$.

4. Methods and Qualitative Analysis

Systems of ordinary differential equations are used to mathematically simulate a variety of scientific and technical problems, and there are several techniques to study the dynamic behavior of state variables. In this paper, we work with three different techniques for the given model. The main concept of IMEXRK is to divide it into two methods: implicit-explicit Runge-Kutta, with the linear component being treated by an implicit scheme and the nonlinear term being treated by an explicit scheme. For more information, see [12, 15]. To make progress, we return to system (1) and concentrate on non-linear systems of ordinary differential equations, applying the concepts detailed in the preceding sections.

$$F\big(t, x(t)\big) = \begin{bmatrix} r_1 - (r_4 + r_2)S(t) \\ -(r_5 + r_2 + r_6 + r_7)E(t) \\ r_4S(t) + r_5E(t) - (r_2 + r_8 + r_9)Q(t) \\ r_7E(t) + r_9Q(t) - (r_2 + r_{12})I_A(t) \\ r_6E(t) + r_8Q(t\,) - (r_{10} + r_2 + r_{11})I_S(t) \\ r_{12}I_A(t) + r_{11}I_S(t) - r_2R(t) \end{bmatrix}, \boldsymbol{G}\big(t, \boldsymbol{x}(t)\big) = \begin{bmatrix} -r_3S(t)E(t) \\ r_3S(t)E(t) \\ 0 \\ 0 \\ 0 \\ 0 \\ 0 \end{bmatrix}.$$

Returning to (1) and substituting earlier equations, this results in:

$$(5) \quad \frac{d\boldsymbol{y}(\boldsymbol{t})}{dt} = \boldsymbol{F}\big(t, \boldsymbol{x}(t)\big) + \boldsymbol{G}\big(t, \boldsymbol{x}(t)\big),$$

where $\boldsymbol{y}(t) = [S(t)\ E(t)\ Q(t) I_A(t)\ I_S(t)\ R(t)]^{\mathrm{T}}$. While the non-stiff portion $G\big(t, x(t)\big)$ is addressed using an explicit Runge-Kutta (ERK), the solution of the stiff component $F\big(t, x(t)\big)$ is produced by using a diagonally implicit Runge-Kutta (DIRK) methodology. In this context, the basis of an implicit-explicit Runge-Kutta (s-stage ERK) method is formed by both the s-stage ERK and DIRK procedures using comparable weighting coefficients, indicated as i, where $i = 1,2,\dots,s$.

c_1	a_{11}	0	0	⋯	0	$\hat{c}_1$	0	0	0	⋯	0
c_2	a_{21}	a_{22}	0	⋯	0	$\hat{c}_2$	$\hat{a}_{21}$	0	0	⋯	0
c_3	a_{31}	a_{32}	a_{33}	⋯	0	$\hat{c}_3$	$\hat{a}_{31}$	$\hat{a}_{32}$	0	⋯	0
⋮	⋮	⋮	⋮	⋱	⋮	⋮	⋮	⋮	⋮	⋱	⋮
c_s	a_{s1}	a_{s2}	a_{s3}	⋯	a_{ss}	$\hat{c}_s$	$\hat{a}_{s1}$	$\hat{a}_{s2}$	$\hat{a}_{s3}$	⋯	0
	b_1	b_2	b_3	⋯	b_s		$\hat{b}_1$	$\hat{b}_2$	$\hat{b}_3$	⋯	$\hat{b}_s$

A more concise expression of this could possibly be achieved with the Kronecker product.

$c^{[I]}$	$\mathcal{A}^{[I]}$	$c^{[E]}$	$\mathcal{A}^{[E]}$
	$(b^{[I]})^T$		$(b^{[E]})^T$

The symbols [I] and [E] are employed to denote the implicit along explicit elements, respectively, inside the sentence. The term $\boldsymbol{y}^{n+1}$, which is estimated using the following method, has been defined as:

$$\boldsymbol{y}^{n+1} = \boldsymbol{y}^n + \Delta t \sum_{i=1}^{s} b_i \boldsymbol{k}_i \text{, where}$$

$$\boldsymbol{k}_i = \boldsymbol{F}\left(t + \Delta t, \boldsymbol{y}^n + \Delta t \sum_{j=1}^{i} a_{ij} k_j\right) + \boldsymbol{G}\left(t + \Delta t, \boldsymbol{y}^n + \Delta t \sum_{j=1}^{i-1} \hat{a}_{ij} k_j\right), i = 1,2, \dots, s.$$

Table 2 shows the coefficients of our IMEX-RK (4,5,5) technique, which is a 5-stage IERK approach with fourth-order accuracy.

Table 2**:** Fourth-order implicit-explicit Runge-Kutta technique coefficients IMEX-RK (4,5,5).

c_1	1/4	0	0	0	0
c_2	0.34114705729739	1/4	0	0	0
c_3	0.80458720789763	−0.07095262154540	1/4	0	0
c_4	−0.52932607329103	1.15137638494253	−0.80248263237803	1/4	0
c_5	0.11933093090075	0.55125531344927	−0.1216872844994	0.20110104014943	1/4
	0.11933093090075	0.55125531344927	−0.1216872844994	0.20110104014943	1/4

and

$\hat{c}_1$	0	0	0	0	0
$\hat{c}_2$	0.39098372452428	0	0	0	0
$\hat{c}_3$	1.09436646160460	0.33181504274704	0	0	0
$\hat{c}_4$	0.14631668003312	0.69488738277516	0.46893381306619	0	0
$\hat{c}_5$	−1.33389883143642	2.90509214801204	−1.06511748457024	0.27210900509137	0
	0.11933093090075	0.55125531344927	−0.1216872844994	0.20110104014943	1/4

5. Analysis of COVID-19 Disease Systems

At the levels of the variables that cause the rates of change to become zero, we say that the system is in equilibrium. These coordinates stand for a steady condition when the system does not change. Points of equilibrium in our COVID-19 illness model would be when there is no longer any change in the numbers of people in each compartment. The existence of many equilibrium points might lead to

various consequences for disease dynamics. To determine the equilibrium points, we may solve the system (1) by setting every rate of change equation to zero, then calculating for the relevant variables.

$$\frac{dS(t)}{dt} = \frac{dE(t)}{dt} = \frac{dQ(t)}{dt} = \frac{dI_{A(t)}}{dt} = \frac{dI_{S(t)}}{dt} = \frac{dR(t)}{dt} = 0.$$

We calculated the values of variables S, E, Q, I_A, I_S, and R by equating each component to zero and replacing parameters from Table 1. This identified two equilibrium points:

$E_1 = (2.3491, 0, 2.2350e-2, 2.1181e-2, 6.7436e-4, 1.1564e-4)$ and

$E_2 = (6.5267, -8.5875e-2, 6.1275e-2, -4.8019e-1, -3.6145, \quad -8.3017e-3).$

A large susceptible population (S) and low exposed (E) and quarantined (Q) populations are predicted at the equilibrium point (E_1). Small numbers of asymptomatic (I_A) and symptomatic (I_S) infected people exist. The recovered population (R) is extremely restricted, indicating a managed sickness where most individuals are susceptible. E, I_A, I_S and R are negative at E_2, the second equilibrium point. Negative numbers are not physically meaningful and may indicate model or calculation errors. Linearization is a useful approach for gaining a deeper understanding of systems around equilibrium points. The eigenvalues and Jacobian matrix may be obtained for every equilibrium point.

The eigenvalues of E_1 were computed, and the resulting values were inserted into the Jacobian matrix (4). The given numeric values

$$(\lambda_1, \lambda_2, \lambda_3, \lambda_4, \lambda_5, \lambda_6) = (-0.0106, -0.0210, -0.0106, -0.0107, -0.3363, -0.0108),$$

if the eigenvalues are negative, then E_1 is considered stable. This stability means the illness may be treated or prevented, possibly by isolation until a vaccine is available. We plot 2D and 3D phase portraits from various viewpoints to analyze the behavior of a system (1). The phase image illustrates the impact of changes in population compartments on others, hence displaying the dynamics of the system. Comparing many groups allows researchers to get insight into the stability and behavior of the system under different conditions. In epidemiology, this knowledge is fundamental for creating efficient treatments and control techniques. We determine the stability behavior for these components by plotting a 2D for the number of exposed vs susceptible, susceptible vs quarantined, quarantined vs exposed, and asymptomatic vs symptomatic infected persons. And we plot a 3D since the 3D phase portrait offers a thorough understanding of the dynamic behavior of the epidemiological system. The stability and long-term behavior of the system may be understood by examining the vector field and trajectories, which can assist in guiding the development of disease control measures. First, we plot the group of ($S, E,$ and Q) and then (I_A, I_S and R) for analyzing the relationship between them, so we will discuss more about it in section 7.

6. Sensitivity Analysis

One of the best ways to better comprehend the dynamics of the biological system and investigate the mathematical model's output is sensitivity analysis via the mass action law. The sensitivity analysis method formulation with m reversible reactions and n components are simply presented below:

$$\sum_{j=1}^{n} \alpha_{ij} \mathcal{C}_j \underset{\mathcal{R}_i^b}{\overset{\mathcal{R}_i^f}{\rightleftharpoons}} \sum_{j=1}^{n} \beta_{ij} \mathcal{C}_j, \quad i = 1,2, \dots, m, \tag{6}$$

The elements of $\mathcal{C}_j$, where j ranges from 1 to n, are represented by α_{ij} and β_{ij}, which are integers that are non-negative. The reactions, both forward as well as backward, are always occurring with $R_i^f > 0$ and $R_i^b \geq 0$. The response rates may be determined by using the mass action formula.

$$r_i = \mathcal{R}_i^f \prod_{j=1}^{n} \mathcal{C}_j^{\alpha_{ij}}(t) - \mathcal{R}_i^b \prod_{j=1}^{n} \mathcal{C}_j^{\beta_{ij}}(t). \tag{7}$$

Therefore, the system of DEqs is shown as follows

$$\frac{d\mathcal{C}}{dt} = \sum_{i \in J \subset \mathbb{R}} \gamma_i \, r_i \,, \tag{8}$$

Where $\gamma_i = \beta_{ij} - \alpha_{ij}$, for $i = 1,2, \dots, m$ and $j = 1,2, \dots, n$. Equation (8) may be expressed as follows:

$$\frac{d\mathcal{C}_j}{dt} = \ell_j(\mathcal{C}, \mathcal{R}), \tag{9}$$

Where $\mathcal{C} \in \mathbb{R}^n$ and $\mathcal{R} \in \mathbb{R}^m$. The vector of elements serves as the inputs as well as the outcomes of the model [16, 17]. Moreover, local sensitivity refers to the variation in the model variables $\mathcal{C}_j, j = 1,2, \dots, n$ with respect to the parameters of the model $\mathcal{R}_p,\ p = 1,2, \dots, m$. The sensitivity model formula for each variable with respect to the parameters is often written as follows:

$$\mathcal{S}_{jp} = \frac{\partial \mathcal{C}_j}{\partial \mathcal{R}_p} = \lim_{\Delta \mathcal{R}_p \to 0} \frac{\mathcal{C}_j(\mathcal{R}_p + \Delta \mathcal{R}_p) - \mathcal{C}_j(\mathcal{R}_p)}{\Delta \mathcal{R}_p} \tag{10}$$

Equation (5.5) could be computed by the finite difference approach in the following way.

$$\mathcal{S}_{jp} = \frac{\partial \mathcal{C}_j}{\partial \mathcal{R}_p} \approx \frac{\mathcal{C}_j(\mathcal{R}_p + \Delta \mathcal{R}_p) - \mathcal{C}_j(\mathcal{R}_p)}{\Delta \mathcal{R}_p} \tag{11}$$

In essence, direct analysis of sensitivity is conducted to formulate the sensitivity formula, which requires solving DEqs for sensitivity coefficients.

$$\frac{\partial \mathcal{S}_{jp}}{\partial t} = \frac{\partial}{\partial t}\left(\frac{\partial \mathcal{C}_j}{\partial \mathcal{R}_p}\right) = \frac{\partial}{\partial \mathcal{R}_p}\left(\frac{\partial \mathcal{C}_j}{\partial t}\right) = \frac{\partial}{\partial \mathcal{R}_p}\Big(\ell_j(\mathcal{C}(t), \mathcal{R})\Big). \tag{12}$$

Thus, the Jacobian matrix is applied in the local sensitivity expression in the following ways:

$$\dot{\mathcal{S}} = \mathcal{L}_{\mathcal{R}_p} + \mathcal{J}.\mathcal{S},\ \ p = 1,2, \dots, m, \tag{13}$$

The matrices $\mathcal{S}, \mathcal{L}_{\mathcal{R}_p}$ and $\mathcal{J}$ are given below.

$$\mathcal{S} = \begin{pmatrix} \frac{\partial \mathcal{C}_1}{\partial \mathcal{R}_p} \\ \frac{\partial \mathcal{C}_2}{\partial \mathcal{R}_p} \\ \vdots \\ \frac{\partial \mathcal{C}_n}{\partial \mathcal{R}_p} \end{pmatrix}, \qquad \mathcal{L}_{\mathcal{R}_p} = \begin{pmatrix} \frac{\partial \ell_1}{\partial \mathcal{R}_p} \\ \frac{\partial \ell_2}{\partial \mathcal{R}_p} \\ \vdots \\ \frac{\partial \ell_n}{\partial \mathcal{R}_p} \end{pmatrix}, and \ \ \mathcal{J} = \begin{pmatrix} \frac{\partial \ell_1}{\partial \mathcal{C}_1} & \frac{\partial \ell_1}{\partial \mathcal{C}_2} & \cdots & \frac{\partial \ell_1}{\partial \mathcal{C}_n} \\ \frac{\partial \ell_2}{\partial \mathcal{C}_1} & \frac{\partial \ell_2}{\partial \mathcal{C}_2} & \cdots & \frac{\partial \ell_2}{\partial \mathcal{C}_n} \\ \vdots & \vdots & \ddots & \vdots \\ \frac{\partial \ell_n}{\partial \mathcal{C}_1} & \frac{\partial \ell_n}{\partial \mathcal{C}_2} & \cdots & \frac{\partial \ell_n}{\partial \mathcal{C}_n} \end{pmatrix}.$$

The initial conditions for the system (5.8) are computed by entering parameters $\mathcal{R}_p$ and initial conditions for output components $\mathcal{C}_j$. Readers might find further information in [17, 18]. The Symbiology Toolbox in MATLAB allows for the computation of local sensitivity values in equation (13) using three distinct methods: complete normalization, half normalization, and non-normalization. For complex modeling situations, such as the coronavirus, it is essential to thoroughly and precisely prioritize sensitivity analysis. Consequently, we have a look at the coronavirus equations from system (1) and determine the local sensitivity of the model compartments to the model parameters in three separate cases. These results are shown in Figures (4-6).

7. Numerical Results

The purpose of this part is to demonstrate the usefulness and effectiveness of a certain method by implementing a numerical solution using MATLAB. In this section, we use two different computation techniques: the Implicit-Explicit Runge-Kutta (IMEX-RK) approach has a setup of (4, 5, 5), and the conventional Explicit Runge-Kutta (ERK) approach. The purpose of this part is to demonstrate the usefulness and effectiveness of a certain method by implementing a numerical solution using MATLAB. This section will employ two distinct computational methods: the Implicit-Explicit Runge-

Kutta (IMEX-RK) approach, characterized by a configuration of (4, 5, 5), and the traditional Explicit Runge-Kutta (ERK) methodology. The tactics will be used to tackle the system delineated in equation (1). In this context, the numbers 4 and 5 represent the numerical scheme's order and the number of steps for both implicit and explicit procedures, respectively. The starting populations, as well as parameter data in this research, are sourced through the health organization with Nigerian centers of control of illnesses as documented in [3].

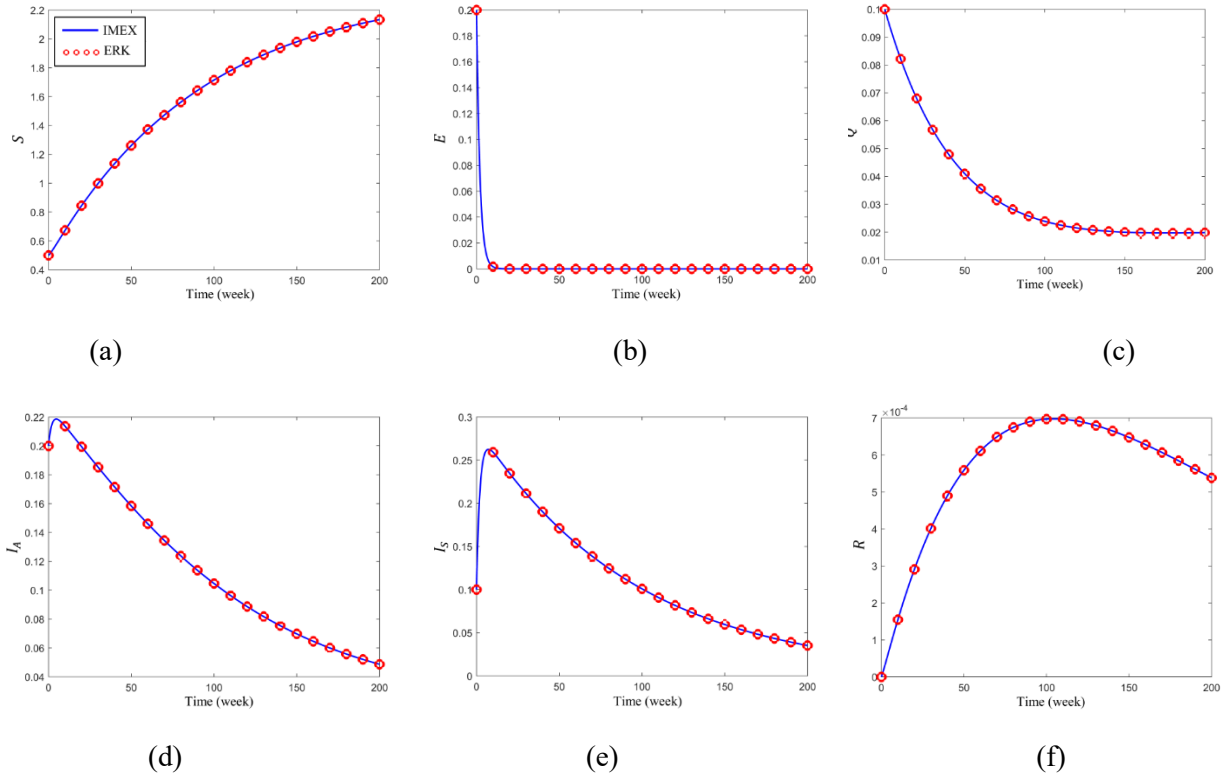

Figure 3: Numerical approximation solutions for the COVID-19 model system (1) in Nigeria using IMEX-RK (4,5,5) and classical Runge-Kutta. (a) Describes the variety of populations that are susceptible (S), (b) populations that were exposed (E), (c) quarantined groups (Q), (d) asymptomatically infected groups (I_A), (e) symptomatically infected populations (I_S), and (f) recovered groups of people (R).

Table 3: Comparison of Classical Runge-Kutta and IMEX-RK (4, 5, 5) Fourth-Order Techniques.

Time (week)	Classical Runge-Kutta of order four			IMEX-RK (4,5,5)		
	$h = 0.01$			$h = 1$		
	$\boldsymbol{S}$	$\boldsymbol{E}$	$\boldsymbol{Q}$	$\boldsymbol{S}$	$\boldsymbol{E}$	$\boldsymbol{Q}$
0	0.5	0.2	0.1	0.5	0.2	0.1
20	0.844549	1.611131 e-05	6.796845 e-02	0.844477	2.359809 e-05	6.797030 e-02
40	1.136823	2.187407 e-09	4.792545 e-02	1.136760	4.492074 e-09	4.792754 e-02
60	1.372321	4.534481 e-13	3.561369 e-02	1.372267	1.263021 e-12	3.561558 e-02
80	1.562069	1.321962 e-16	2.821411 e-02	1.562023	4.869289 e-16	2.821564 e-02
100	1.714956	5.072652 e-20	2.390735 e-02	1.714917	2.423082 e-19	2.390851 e-02
120	1.838143	2.428817 e-23	2.152444 e-02	1.838110	1.481955 e-22	2.152527 e-02
140	1.937399	1.390020 e-26	2.031848 e-02	1.937371	1.070604 e-25	2.031904 e-02
160	2.017373	9.184695 e-30	1.981575 e-02	2.017349	8.847147 e-29	1.981612 e-02

180	2.081810	6.813972 e-33	1.971869 e-02	2.081791	8.148628 e-32	1.971891 e-02
200	2.133730	5.549553 e-36	1.984277 e-02	2.133714	8.191531 e-35	1.984288 e-02

Table 4: Comparison of Classical Runge-Kutta and IMEX-RK (4, 5, 5) Fourth-Order Techniques.

Time (week)	Classical Runge-Kutta of order four			IMEX-RK (4,5,5)		
	$h = 0.01$			$h = 1$		
	I_A	I_S	R	I_A	I_S	R
0	0.2	0.1	0	0.2	0.1	0
20	0.199441	0.234744	2.907360 e-04	0.199448	0.234797	2.907026 e-04
40	0.171490	0.190114	4.897543 e-04	0.171497	0.190163	4.897440 e-04
60	0.146037	0.153930	6.110213 e-04	0.146043	0.153970	6.110270 e-04
80	0.123727	0.124622	6.746733 e-04	0.123732	0.124655	6.746895 e-04
100	0.104667	0.100897	6.969194 e-04	0.104671	0.100924	6.969425 e-04
120	8.867742 e-02	8.169795 e-02	6.904617 e-04	8.868103 e-02	8.171998 e-02	6.904889 e-04
140	7.544328 e-02	6.616693 e-02	6.650216 e-04	7.544642 e-02	6.618493 e-02	6.650511 e-04
160	6.460206 e-02	5.360659 e-02	6.278741 e-04	6.460478 e-02	5.362131 e-02	6.279044 e-04
180	5.579220 e-02	4.345094 e-02	5.843379 e-04	5.579455 e-02	4.346297 e-02	5.843680 e-04
200	4.867884 e-02	3.524104 e-02	5.382016 e-04	4.868085 e-02	3.525088 e-02	5.382307 e-04

8. Discussion and Conclusion

The health care program needs a full understanding of the transmission of infectious diseases for controlling or preventing them, and to properly understand, we need mathematical modeling and computational simulations. Theoretical investigation into such models supports biologists in order to predict model behaviors and identify important parameters of the model. First, we proved that the solution of system (1) exists and is unique, then we employed the IMEX-RK technique to compute numerical approximations for the COVID-19 differential equation system, incorporating both stiff and non-stiff components. The implicit scheme handles the stiff segment, while the explicit scheme manages the other portion. A key focus of our approach is diminishing iteration count, thereby lowering the computational burden. The results unequivocally demonstrate the superiority of our method over the classical Runge-Kutta method in stability and computational efficiency.

Therefore, we have computed approximate solutions for each state of the model using the reported cases, see Figure 3. These calculations mark a substantial stride forward in pinpointing pivotal elements within the model and charting the course for prospective enhancements. The computational outcomes acquired have the potential to bolster global initiatives focused on mitigating the impact of the ailment on individuals and facilitating the implementation of broader strategies for curbing the transmission of the coronavirus within communities. Additionally, in our stability analysis, we have discerned a stable point, signifying that at this juncture, the disease exhibits stability. This finding underscores the effectiveness of containment measures, such as quarantine or direct vaccination, in controlling the disease's further dissemination.

Consequently, we have calculated a phase portrait in 2D dimensions for S vs E, S vs Q, E vs Q, and I_A vs , I_S which is presented in Figure 4. The plots' red arrows show which way the system is moving in phase space. And about their behavior, these trajectories imply the existence of equilibrium sites, or attractors, where the system gradually stabilizes. And the nonlinear character of these correlations points to intricate interactions between the model's various compartments, which is characteristic in epidemiological models where a variety of factors influence the transmission of disease. These phase

portraits show how modifications in one population compartment impact other population compartments, offering insight into the system's dynamics. To create efficient interventions and control techniques in epidemiology, researchers must first understand the stability and behavior of the system under various conditions, which can be accomplished by examining these plots. And the 3D phase portrait for $S, E,$ and Q together and I_A, I_S and R together presented in Figure 5), shows that the system's vector field, represented by the red arrows, shows the motion and rate of change of the variables, and illustrates the way a system changes over time. And the blue curve represents a trajectory or a solution for the system. This trajectory shows how the variables vary with time, beginning at a specific initial state. Figure 5 (I) illustrates that while the number of susceptible people decreases the number of the number of exposed people increases and then stabilizes, meanwhile the number of individuals from quarantine people are increases. And from the whole 3D phase portrait, it's clear that the system will eventually stabilize. And Figure 5(II) demonstrates that at first, the number of asymptomatic infected people rises while that of symptomatic infected people declines. There is a gradual increase in the number of recovered individuals, suggesting that people progress through stages of infection to recovery. The trajectory indicates that populations that are asymptomatic, symptomatic, and recovered eventually lead to stabilization. Understanding the stability and long-term behavior of the system is essential for comprehending the dynamics of disease progression and recovery. This can be achieved by evaluating the vector field and trajectories. Public health policies for controlling transmission and recovery from infectious diseases can benefit from this approach.

Incorporating the principle of local sensitivity analysis, as outlined in equation (13), represents a pivotal advancement in our quest for further exploration and model refinement. The calculation of local sensitivity concerning each model compartment in relation to model parameters necessitates the utilization of the Symbiology Toolbox within MATLAB. We employ three distinct methodologies to assess the sensitivities of these models: full normalizations, half normalizations, and non-normalizations, as illustrated in Figures 4-6. Remarkably, these results not only enhance our comprehension of the model but also enable us to identify the pivotal parameters critical to its performance. Figure 6 clearly illustrates that the group of parameters $\{r_1, r_6, r_7\}$ exhibits the highest level of sensitivity concerning the dynamics of COVID-19. Particularly, r_6 which represents the rate of transition from the exposed class to symptomatic infected individuals' class, demonstrates a remarkably strong sensitivity to the state variable E, representing the population of exposed individuals. In contrast, the parameters $\{r_2, r_3, r_4, r_5, r_8, r_9, r_{10}, r_{11}, r_{12}\}$ appear to have a less pronounced impact on the overall model. Figure 7 provides us with the model parameters $r_2, r_3, r_5, r_6, r_7, r_8, r_9, r_{10}, r_{11}$ and r_{12} are the least critical, especially r_3 is very sensitive for all state variables, but r_1 and r_4 are typically critical to a model, especially r_4 is very sensitive to the state variable Q (Quarantined individuals). Figure 8 also shows that the group $\{r_3, r_5, r_6, r_7, r_8, r_9, r_{10}, r_{11}, r_{12}\}$ model parameters are the lowest critical, whilst the set of model parameters $\{r_1, r_2, r_4\}$ becoming sensitive to the model states, especially r_1 (Rate of recruiting), it is very sensitive to the state variable S (Susceptible individuals).

Therefore, employing computational simulations to pinpoint the pivotal parameters of the model under examination proves to be a highly efficient approach for comprehensively exploring the model, both in practical and theoretical contexts. Furthermore, this method allows for the formulation of recommendations aimed at advancing future endeavors in the field of coronavirus prevention, encompassing vaccination strategies, treatment modalities, and disease control measures.

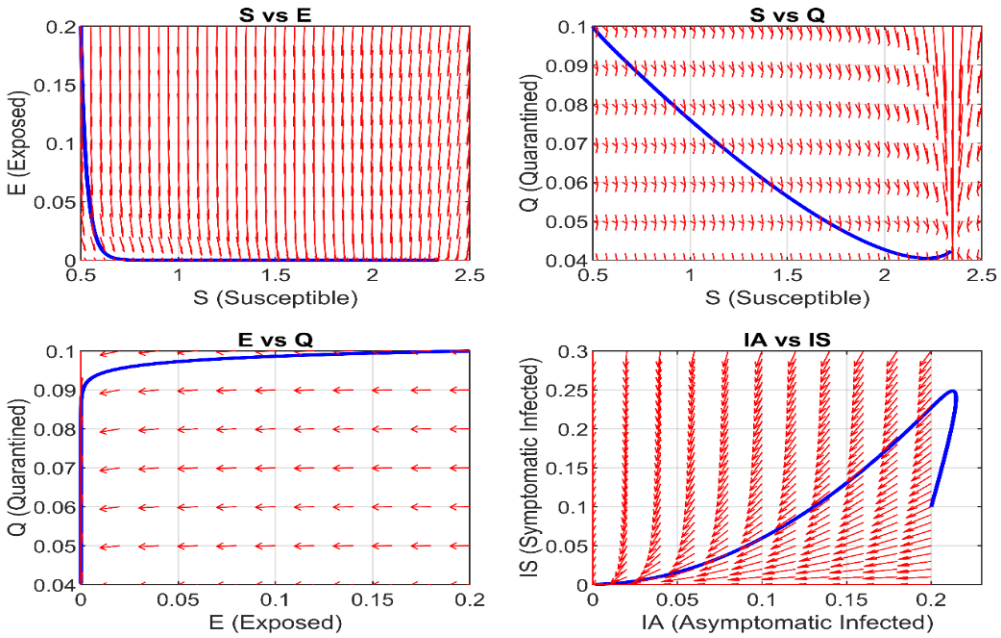

Figure 4: The relationship between two important variables is shown in each plot: S vs E, indicating a sharp decline in those who are exposed while the number of those who are susceptible rises and then levels off. S vs Q: Shows a decline in those placed under quarantine as the number of susceptible people rises; the curve is steep at first and then becomes more rounded. E vs Q: Shows a dramatic increase in those under quarantine as the number of exposed people rises, leveling off at an equilibrium level. I_A *vs* I_S: Shows a nonlinear relationship in which a rise in asymptomatic people eventually causes a fall in symptomatic people.

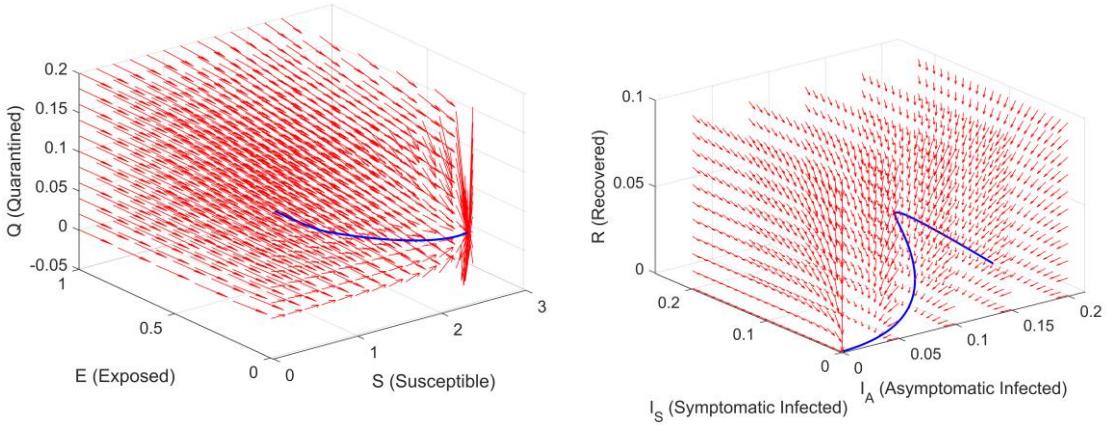

(I) (II)

Figure 5**:** The 3D phase portrait illustrates the dynamics of infectious disease spread and control techniques by showing the interactions between: (I) susceptible (S), exposed (E), and quarantined (Q) individuals in an epidemiological system. (II) Asymptomatic infected (I_A), Symptomatic infected (I_S) and recovered individuals R inside a system of epidemiology.

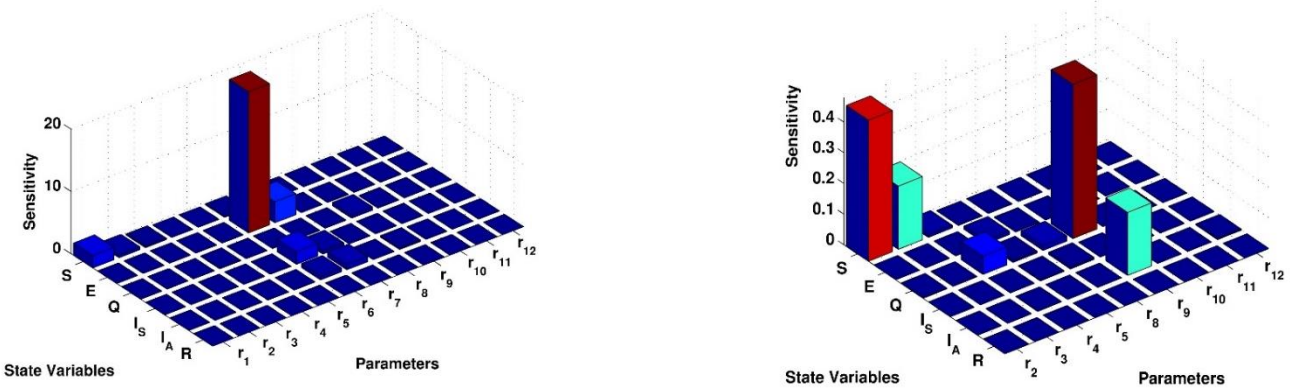

(I) (II)

Figure 6: The two figures are local sensitivity analyses for COVID-19 computed with full normalizations by using MATLAB in this approach, the group of parameters $\{r_1, r_6, r_7\}$ extremely sensitive compared with other parameters, especially r_6 is very sensitive to the state variable E (Exposed individuals), (I) Evaluating the responsiveness of all compartments to various parameters. (II) Assessing the sensitivity of all compartments to parameters, excluding $\{r_1, r_6, r_7\}$.

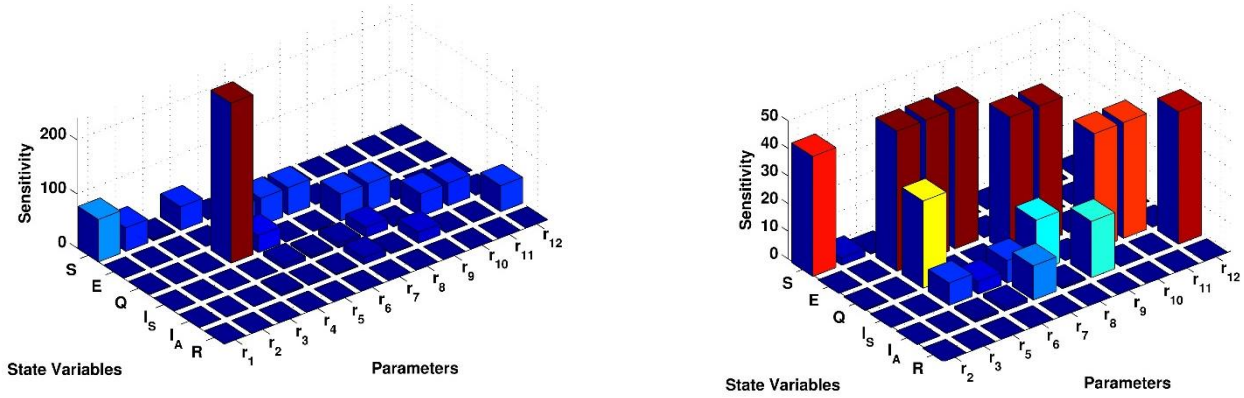

(I) (II)

Figure 7: Tne two figures are local sensitivity analyses for COVID-19 computed with half normalizations by using MATLAB; in this approach, both parameters r_1 and r_4 are very sensitive compare with other parameters, especially r_4 is very sensitive to the state variable Q (Quarantined individuals), in both figures r_3 is very little sensitive to all state variables, (I) evaluation of the sensitivity of all compartments concerning various parameters. (II) Assessment of the sensitivity of all compartments concerning various parameters, excluding r_1 and r_4.

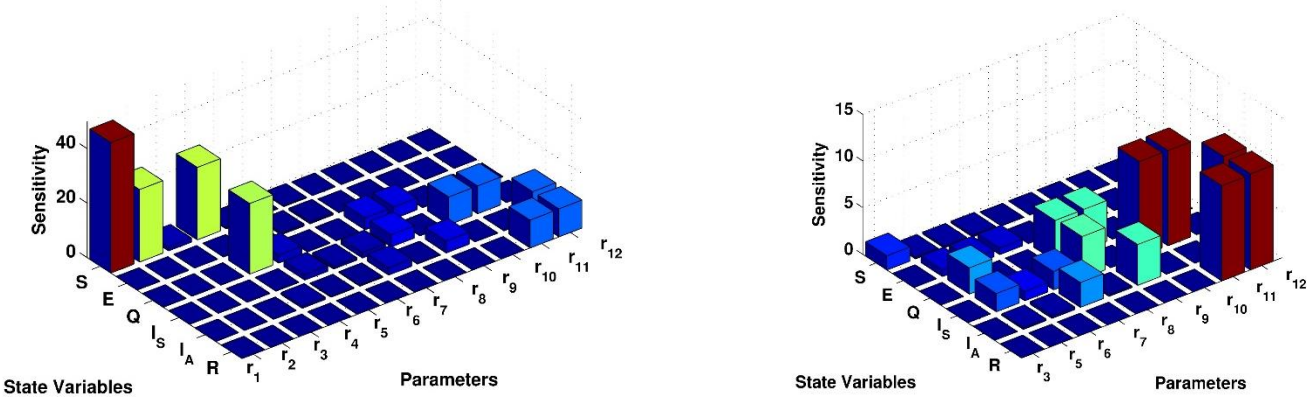

(I) (II)

Figure 8: The two figures are local sensitivity analysis for COVID-19 computed with non-normalizations by using MATLAB, in this approach, the group of parameters $\{r_1, r_2, r_4\}$ are very sensitive compare with other parameters, especially r_1 is very sensitive to the state variable S (Susceptible individuals), (I) Analysis of the sensitivity of all compartments in relation to all parameters. (II) Examination of the sensitivity of all compartments with respect to the set of parameters $\{r_3, r_5, r_6, r_7, r_8, r_9, r_{10}, r_{11}, r_{12}\}$.

Acknowledgments

The authors gratefully acknowledge the academic and institutional support provided by Koya University.

Funding

Not applicable.

Author's Contribution

Hemn Mohammed Rasool conceived the main idea of the paper and wrote the abstract, introduction, model formulation, mathematical model, methods, sensitivity analysis with simulations, result discussion, and conclusion. Berivan Faris Azeez improved the manuscript through paraphrasing and refinement. Mardan Ameen Pirdawood prepared the numerical section, carried out its simulations, and proved the existence and uniqueness of the system. All authors approved the final manuscript.

Conflict of interest

The authors declare that there is no conflict of interest.

Data availability statement

Not applicable.

Informed consent statement

Not applicable.

Ethical approval statement

Not applicable.

References

[1] Zhu N, Zhang D, Wang W, Li X, Yang B, Song J, et al. A novel coronavirus from patients with pneumonia in China, 2019. New England journal of medicine. 2020;382(8):727-33. https://doi/org/10.1056/NEJMoa2001017

[2] Dai Y, Wang J. Identifying the outbreak signal of COVID-19 before the response of the traditional disease monitoring system. PLoS neglected tropical diseases. 2020;14(10):e0008758. https://doi/org/10.1371/journal.pntd.0008758

[3] Ahmed I, Modu GU, Yusuf A, Kumam P, Yusuf I. A mathematical model of Coronavirus Disease (COVID-19) containing asymptomatic and symptomatic classes. Results in Physics. 2021;21:103776. https://doi/org/10.1016/j.rinp.2020.103776

[4] Koo JR, Cook AR, Park M, Sun Y, Sun H, Lim JT, et al. Interventions to mitigate early spread of SARS-CoV-2 in Singapore: a modelling study. The Lancet Infectious Diseases. 2020;20(6):678-88. https://doi/org/10.1016/S1473-3099(20)30162-6

[5] Okuonghae D, Omame A. Analysis of a mathematical model for COVID-19 population dynamics in Lagos, Nigeria. Chaos, Solitons & Fractals. 2020;139:110032. https://doi/org/10.1016/j.chaos.2020.110032

[6] Ogundokun RO, Lukman AF, Kibria GBM, Awotunde JB, Aladeitan BB. Predictive modelling of COVID-19 confirmed cases in Nigeria. Infectious Disease Modelling. 2020;5:543-8. https://doi/org/10.1016/j.idm.2020.08.003

[7] Adegboye OA, Adekunle AI, Gayawan E. Early transmission dynamics of novel coronavirus (COVID-19) in Nigeria. International Journal of Environmental Research and Public Health. 2020;17(9):3054. https://doi/org/10.3390/ijerph17093054

[8] Ajisegiri W, Odusanya O, Joshi R. COVID-19 outbreak situation in Nigeria and the need for effective engagement of community health workers for epidemic response. Global Biosecurity. 2020;1(4). https://doi/org/10.31646/gbio.69

[9] Khoshnaw SH, Rasool HM, editors. Mathematical Modelling for complex biochemical networks and identification of fast and slow reactions. The international conference on mathematical and related sciences; 2019: Springer. https://doi/org/10.1007/978-3-030-43002-3

[10] Akgül A, Khoshnaw SH, Rasool HM. Minimizing cell signalling pathway elements using lumping parameters. Alexandria Engineering Journal. 2020;59(4):2161-9. https://doi/org/10.1016/j.aej.2020.01.041

[11] Khoshnaw SH, Rasool HM. Entropy production and lumping of species can effectively reduce complex cell signaling pathways. Physica Scripta. 2022;97(5):054006. https://doi/org/10.1088/1402-4896/ac6211

[12] Pirdawood MA, Rasool HM, Sabawi YA, Azeez BF. Mathematical Modeling and Analysis for COVID-19 Model by Using Implicit-Explicit Rung-Kutta Methods. Academic Journal of Nawroz University. 2022;11(3):65-73. https://doi/org/10.25007/ajnu.v11n1a1244

[13] Sabawi YA, Pirdawood MA, Rasool HM, Ibrahim S, editors. Model Reduction and Implicit–Explicit Runge–Kutta Schemes for Nonlinear Stiff Initial-Value Problems2023; Singapore: Springer Nature Singapore. https://doi/org/10.1007/978-981-99-0447-1_9

[14] Giordano P, Baglini LL. A Picard-Lindel\" of theorem for smooth PDE. arXiv preprint arXiv:221101118. 2022. https://doi/org/10.48550/arXiv.2211.01118

[15] Asif M, Khan ZA, Haider N, Al-Mdallal Q. Numerical simulation for solution of SEIR models by meshless and finite difference methods. Chaos, Solitons & Fractals. 2020;141:110340. https://doi/org/10.1016/j.chaos.2020.110340

[16] Pirdawood MA, Rasool HM, Aziz BF. Integrating Sensitivity Analysis and Explicit Runge-Kutta Method for Modeling the Effect of Exposure Rate to Contaminated Water on Cholera

Disease Spread. Passer Journal of Basic and Applied Sciences. 2023;6(1):33-41. https://doi/org/10.24271/psr.2023.412783.1375

[17] Powell DR, Fair J, LeClaire RJ, Moore LM, Thompson D, editors. Sensitivity analysis of an infectious disease model. Proceedings of the international system dynamics conference; 2005. https://doi/org/10.665-3839/CA.95054

[18] Zi Z. Sensitivity analysis approaches applied to systems biology models. IET systems biology. 2011;5(6):336-46. https://doi/org/10.1049/iet-syb.2011.0015